Chinese Physics Letters **42**, 057301 (2025) **Express Letter**

Dynamics in the Planar Pyrochlore Lattice: Flat Band, Domain Wall, and Anomaly

Zijian Xiong[1,2,3], Yining Xu[1*], and Xue-Feng Zhang[2,3*]

[1]*College of Physics and Electronic Engineering, Chongqing Normal University, Chongqing 401331, China*
[2]*Department of Physics, and Center of Quantum Materials and Devices, Chongqing University, Chongqing 401331, China*
[3]*Chongqing Key Laboratory for Strongly Coupled Physics, Chongqing 401331, China*

(Received 10 February 2025; accepted manuscript online 3 April 2025)

The quantum phase transition between $\mathbb{Z}_2$ plaquette valence bound solid (PVBS) and superfluid (SF) phases on the planar pyrochlore lattice (square ice) is under debate. To gain further insight, here, we focus on the dynamical features of the hard-core Bose–Hubbard model on this lattice and study the excitation spectra by combining stochastic analytic continuation and quantum Monte Carlo simulation. In both PVBS and SF phases, a flat band with bow-tie structure is observed and can be explained by certain symmetries. At the transition point, the spectra turn to be continuous and gapless. A (2+1)-dimensional Abelian–Higgs model with mixed 't Hooft anomaly is proposed to describe the transition, where the anomaly matching predicts that the deconfinement can exist on the domain walls. From the snapshot of the spin configuration in real space, we found the existence of the domain wall. We also found that the spectrum along a specific path in momentum space from PVBS phase to the transition point can be well described by an XXZ spin chain, and the critical theory of XXZ spin chain matches the anomaly. The two-spinon continuum along this specific path implies additional domain walls (point defect) can emerge in the domain walls (line defect) and take the role of deconfinement at the transition point.

DOI: 10.1088/0256-307X/42/5/057301 CSTR: 32039.14.0256-307X.42.5.057301

Introduction. Gauge theories play a vital role in particle physics, but also become a powerful tool to study condensed matter physics. As a fertile ground for seeking the unconventional phases and exotic excitations,[1–3] geometrical frustration usually leads to the local constraint for the semi-classical ground states, which can often be formulated as an emergent gauge theory[2,3] and gives rise to extensive degeneracy. As a paradigmatic example, the pyrochlore quantum spin ice manifesting emergent U(1) gauge structure,[4,5] and the corresponding effective field theory is QED_4.[6]

In comparison, the effective field theory depicting a two-dimensional frustrated system could be QED_3, and a straightforward example is the two-dimensional spin ice – planar pyrochlore lattice (Fig. 1). The Ising model in this lattice is equivalent to the six-vertex model and was exactly solved by Lieb,[7] the ground state is extensively degenerate and all correlation functions are found to decay algebraically. When the quantum fluctuation is introduced,[8–12] the degeneracy will be lifted, and the ground state becomes a PVBS phase which breaks translational symmetry. On the other hand, in the free particle limit, a flat band physics will naturally emerge due to the lattice geometry.[13] However, the phase transition between them is still controversial.[11,14] Importantly, the planar pyrochlore lattice has been experimentally realized in the Rydberg atoms array[15,16] and superconducting qubits systems.[17,18] Thus, as an experimentally achievable mixture of flat band physics and emergent low-dimensional gauge field, the quantum many-body physics in the planar pyrochlore lattice becomes more appealing.

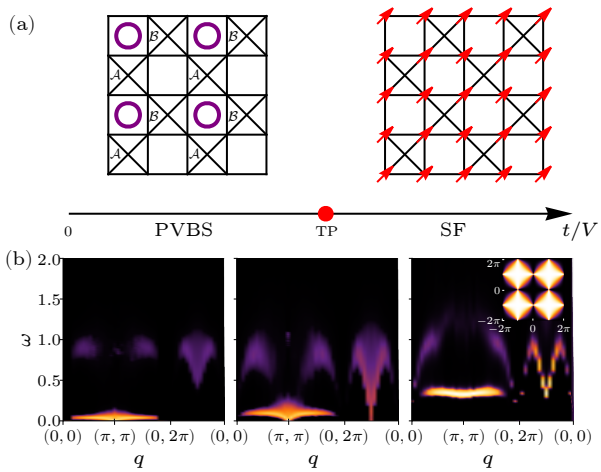

Fig. 1. (a) Phase diagram and the schematic depiction of PVBS (left) and SF (right) phases. The flippable plaquettes are denoted by purple circles, and the centers of the crossing plaquette compose the dual lattice with sublattices $\mathcal{A}$ and $\mathcal{B}$. The TP is marked with a red point. (b) The spectra of the PVBS phase (left), TP (middle) and SF (right) phase (Inset: the bow-tie flat band calculated by spin wave theory with constant energy cut).

*Corresponding author. Email: xuyining@cqnu.edu.cn; zhangxf@cqu.edu.cn
© 2025 Chinese Physical Society and IOP Publishing Ltd. All rights, including for text and data mining, AI training, and similar technologies, are reserved.

On the other hand, the rapid developments of field theory provide some powerful approaches, especially the Lieb-Schultz-Mattis-Oshikawa-Hastings (LSMOH) theorem which restricts the possible ground states.[19–23] Recently, it has been further reinterpreted as one type of mixed 't Hooft anomaly.[24–30] And such non-perturbative anomaly matching condition becomes useful in the contexts of deconfined quantum criticality[26,31–34] and also symmetry protected topological phases.[35–37]

In this manuscript, we study the dynamics of the half-filled extended hard-core Bose–Hubbard model in the planar pyrochlore lattice by combining quantum Monte Carlo (QMC) simulations and stochastic analytic continuation (SAC).[38,39] As shown in Fig. 1, away from the transition point, a flat band with bow-tie structure can be found in the low energy part and explained by certain symmetries. As an indication of fractional excitation, the continuous spectra stably appear in the high energy part. Especially close to the transition point (TP), gapless continuous spectra can be observed along the path $(0, 2\pi) \to (0, 0)$ in the momentum space. These exotic phenomena are consistent with the mixed 't Hooft anomaly, and may herald an alternative form of deconfined criticality.

Model and Effective Theory. In the spin language, the model is equivalent to spin-$\frac{1}{2}$ XXZ model via conventional mapping $S_i^+ \to b_i^\dagger$, $S_i^- \to b_i$, $S_i^z \to n_i - 1/2$:

$$H = -t \sum_{\langle i,j \rangle} (S_i^+ S_j^- + S_i^- S_j^+) + V \sum_{\langle i,j \rangle} S_i^z S_j^z, \qquad (1)$$

where t, $V > 0$ are the magnitudes of XY and Ising interactions (set $V = 1$ as energy unit), $\langle i, j \rangle$ represents the nearest-neighbor bonds and connected diagonal bonds, as shown in Fig. 1(a). When $t/V = 0$, the ground state is subject to the local constraint $S_{\boxtimes}^z = 0$ [$S_{\boxtimes}^z = \sum_{i \in \boxtimes} S_i^z$ is defined in a crossing plaquette ($\boxtimes$)], because the Ising interaction term can be rewritten as $\frac{V}{2} \sum_{\boxtimes} (S_{\boxtimes}^z)^2$. Analogous to the two-in-two-out ice rule in spin ice, the spins in each crossing plaquette should satisfy the two-spin-up and two-spin-down condition, so that the ground state is extensively degenerate. In the weak coupling limit $t \gg V$, the spins tend to align in the xy plane and construct the ferromagnetic phase which breaks the U(1) symmetry [superfluid (SF) phase in bosonic representation].

In the strong coupling region $t \ll V$, the effective perturbative ring exchange interaction $H_{\text{ring}} = -\frac{4t^2}{V} \sum_{\square} (S_i^+ S_j^- S_k^+ S_l^- + \text{h.c.})$ on the non-crossing plaquette ($\square$) takes the main effect.[12,40] The non-crossing plaquette with alternating up and down spins (referred to as flippable plaquette) has lower energy under H_{ring}, so the ground state has to maximize the number of flippable plaquettes. As a result, the PVBS phase appears with spontaneous translational symmetry breaking. Indeed, the low energy physics can also be understood through lattice gauge theory.[4,5,40–42] As illustrated in Fig. 1(a), the effective electric field can be defined between nearest-neighbor sites in dual lattice by $E_{\text{rr}'} = \epsilon_{\text{r}} S_{\text{rr}'}^z$, where $\epsilon_{\text{r}} = +1(-1)$ in dual sublattice $\mathcal{A}(\mathcal{B})$, and the vector potential $a_{\text{rr}'}$ is introduced by $S_{\text{rr}'}^{\pm} = \exp(\pm \text{i} \epsilon_{\text{r}} a_{\text{rr}'})$. Then the ice rule is equivalent to the Gauss' law: $Q_{\text{r}} = \text{div} E = \epsilon_{\text{r}} S_{\boxtimes}^z$, where Q_{r} is the gauge charge at the dual site r. Based on the U(1) lattice gauge theory in 2+1 dimension, the gauge charges are confined in the PVBS phase without a gapless photon.[40,43]

The transition point between PVBS and SF phases is numerically found $t/V \approxeq 0.065$.[11] Similar to the XXZ model in the Kagome lattice,[44] the system can be described with the easy-plane CP^1 model or Abelian–Higgs model:[45–47]

$$\mathcal{L} = -\frac{1}{4e^2} |\text{d}a|^2 + \sum_{i=1}^{2} |\text{D}_a \phi_i|^2 + m^2 \sum_{i=1}^{2} |\phi_i|^2 + \lambda (|\phi_1|^2 - |\phi_2|^2)^2, \qquad (2)$$

where the first term is the Maxwell term,[4,40] D_a is the covariant derivative and ϕ_i is the matter field. The global symmetries can be listed as following: (1) U(1) symmetry for both charges; (2) $\mathbb{Z}_2$ exchange symmetry $\phi_1 \leftrightarrow \phi_2$; (3) $\mathcal{C}$ charge conjugation symmetry; and (4) $\text{U}(1)_{\text{top}}$ topological symmetry relates to the monopoles. To describe the two fold degenerate PVBS phase, the even monopoles term should be included,[47,48] so that the $\text{U}(1)_{\text{top}}$ symmetry is broken to $\mathbb{Z}_{2,\text{top}}$. Then, the Lagrangian in Eq. (2) can hold the mixed 't Hooft anomaly among the global symmetries. When the domain wall excites between two degenerate ground states of PVBS phase (vacuum states), it also carries an anomaly due to the anomaly inflow mechanism.[47–49] This phenomenon is analogous to the well-understood bulk-boundary correspondence in the symmetry protected topological phases. Domain walls can be regarded as boundaries separating different bulk states. According to the field theoretic analysis, the theory of anomaly makes the following predictions:[47] (1) the domain wall should break the symmetry or be gapless; (2) the domain wall (point defect) on the domain wall (line defect) should be deconfined; and (3) the critical theory satisfied this anomaly of the domain wall is supposed to be a compact boson conformal field theory with $c = 1$.

Phases and Bow-Tie Flat Band. With the improvement of the QMC-SAC technique,[38,50] the dynamical structure factor (DSF) $S^{zz}(\boldsymbol{q}, \omega)$ plays a same distinctive role in the numerical simulation as the neutron inelastic scattering in the experiment,[51] which can detect the exotic quantum phase, but also the excitations especially with the topological features.[52–54] Hence, we adopt the QMC-SAC method to simulate the dynamics of the system which hosts the emergent U(1) lattice gauge field and fractional excitations. In order to achieve the high resolution spectrum reflecting low energy physics, the lattice size is set to $N = 32 \times 32 = 1024$ sites with periodic boundary conditions and the temperature is lower to $T = 1/\beta \approx t^2/V$.

The DSF in SF phase with $t/V = 0.1$ is shown in Fig. 2(a), and it consists of two branches. The higher energy branch exhibits strong momentum dependent dispersion, and a flat band can be clearly observed at the lower energy. However, different from spreading to the whole Brillouin zone, the flat band vanishes along the $\boldsymbol{q}$: $(0, 2\pi) \to (0, 0)$. To have a better understanding, we make use of the linear spin wave theory (SWT),

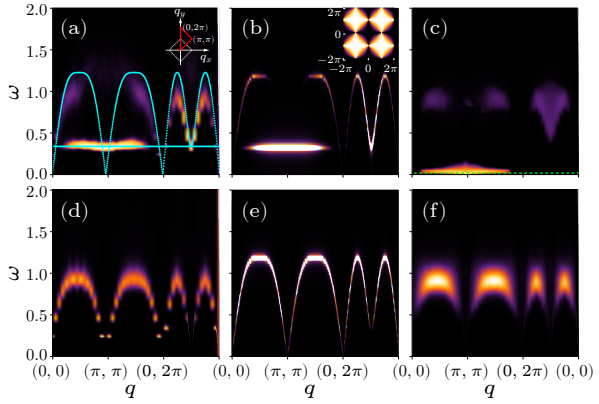

Fig. 2. The DSF $S^{zz}(\boldsymbol{q}, \omega)$ (a)–(c) and the charge-charge correlation spectra $D(\boldsymbol{q}, \omega)$ (d)–(f) in SF phase at $t/V = 0.1$ (a,b,d,e) and PVBS phase at t/V=0.05 (c,f). The spectra of (b,e) are calculated from SWT, while others are from QMC-SAC. The cyan sold lines in (a) are energy dispersion calculated by SWT. The inset in (b) is the constant energy cut of the DSF calculated by SWT with energy ∼0.34 V very close to the flat band. The green dashed line in (c) at $\omega \approxeq 0.02$ is calculated by POT.

and take $t/V = 0.18$ to fit the numerical spectrum, because SWT usually underestimates the quantum fluctuation especially in the geometrically frustrated system.[55] The dispersion can be calculated by diagonalizing the Hamiltonian of the quadratic Holstein-Primakoff bosons $a_{j,\alpha}$, where α is the A,B sublattice index. It is known that the quartic interaction terms in the interacting spin wave theory yield a correction to the dispersion[56] for collinear magnetic order. Here, rather than performing the perturbation theory, we use an effective t/V, which can be regarded as a renormalized coupling from higher order interaction terms. In Fig. 2(a), both flat band and dispersive branches got by SWT (cyan lines) match well with the numerical results. Meanwhile, the DSF from SWT shown in Fig. 2(b) can reproduce many features of the numerical spectra, especially the fragmentation of the flat band. Importantly, after focusing on the energy where flat band resides, a *bow-tie* structure is revealed in the inset of Fig. 2(b), which hints at a possible "selection rule" related to the symmetry.

The planar pyrochlore lattice has the glide reflection symmetries G_x:$(x, y) \to (x+1, -y)$ and G_y:$(x, y) \to (-x, y+1)$.[57] The distance between a $\mathcal{A}$ site and its nearest neighbor $\mathcal{B}$ site is $\sqrt{2}$. Correspondingly, the Holstein-Primakoff bosons follow the transformation: $G_x a_{(q_x,q_y),\alpha} G_x^\dagger = \mathrm{e}^{\mathrm{i}q_x} a_{(q_x,-q_y),\bar{\alpha}}$, $G_y a_{(q_x,q_y),\alpha} G_y^\dagger = \mathrm{e}^{\mathrm{i}q_y} a_{(-q_x,q_y),\bar{\alpha}}$, and $\bar{A} = B$, $\bar{B} = A$. Then, the two eigenmodes of G_y along the $q_x = 0$ path take the form[58] $g_{(0,q_y),\pm} = a_{(0,q_y),A} \pm a_{(0,q_y),B}$, so that the eigenmodes of the Hamiltonian taking Bogoliubov form changes to $b_{(0,q_y),\pm} = u_{(0,q_y),\pm} g_{(0,q_y),\pm} + v_{(0,q_y),\pm} g^\dagger_{(0,-q_y),\pm}$. In real space, the minus mode has alternating sign and constant modulus for sublattice A and B around the non-crossing plaquette, this is known to be the flat mode and originates from the localized excitation.[13,59] Considering $S^z_{\boldsymbol{q}} \propto a_{\boldsymbol{q},A} + a^\dagger_{-\boldsymbol{q},A} + a_{\boldsymbol{q},B} + a^\dagger_{-\boldsymbol{q},B}$ in the SWT, the DSF can only reflect the plus mode. Therefore, the magnitude of the DSF $S^{zz}(\boldsymbol{q}, \omega)$ on the flat band totally vanishes along $q_x = 0$ and $q_y = 0$. Similar "selection rule" behaviors have also been found in the triangular lattice[58] and the kagome lattice.[60]

Same phenomena can also be observed in the PVBS phase, as shown in Fig. 2(c) with $t/V = 0.05$, the flat band branch stays along $\boldsymbol{q}$: $(0, 0) \to (\pi, \pi) \to (0, 2\pi)$ at very low energy and is separated from the high energy continuum by a large gap. Due to the order-from-disorder mechanism, the ring exchange interaction H_{ring} can lift the degeneracy and break the translational symmetry. Thus, the energy scale of the flat band is about $4t^2/V$. A better estimation can be made by plaquette operator theory (POT).[61] In the leading order, we show the dispersion of the lowest excitation with the green dash line in Fig. 2(c). It is flat with energy $\omega \approxeq 0.02$ and corresponds to the excitation from the ground state of an isolated non-crossing plaquette $|e_{\mathrm{g}}\rangle \approx |{\downarrow\uparrow\downarrow\uparrow}\rangle + |{\uparrow\downarrow\uparrow\downarrow}\rangle$ (valid when $t \ll V$) to the first excited state $|e_1\rangle = |{\downarrow\uparrow\downarrow\uparrow}\rangle - |{\uparrow\downarrow\uparrow\downarrow}\rangle$. And the spectral weight of $S^{zz}(\boldsymbol{q}, \omega)$ on the flat band also vanishes along $q_x = 0$ in PVBS, this can be ascribed to a selection rule[60,62,63] from the emergent generalized global symmetries[64,65] in the low energy manifold.

The high energy branches of the PVBS are at the energy scale of V which indicates it may be related to the violation of the ice rule.[66] The charge density can be defined as $m_{\mathrm{r}} = \sum_{i\in\boxtimes_{\mathrm{r}}} S^z_i$, and the ice rule can restrict the Hilbert space to the pure gauge field sector without charge excitation. Then, the quantum fluctuation of emergent gauge field contributes to the flat band. However, the spin exchange interaction can break the ice rule and produce two gauge charges in the same sublattice costing energy V. In order to study the contribution of the gauge charges on the spectrum, we numerically simulate the spectrum of charge density-density correlation $D(\boldsymbol{q}, \omega) = \int_{-\infty}^{\infty} \mathrm{d}t \langle m_{\boldsymbol{q}}(t) m_{-\boldsymbol{q}}(0)\rangle \mathrm{e}^{\mathrm{i}\omega t}$, and also calculate it in SF phase with SWT. From Figs. 2(d)–2(f), we can find the disappearance of the flat band, and it means the high energy branches directly result from the excitation of gauge charge. In the SF phase, the comparison of results from SWT and QMC demonstrates the dispersion of the charge–charge correlation is the same as the dispersive spin wave band. On the other hand, both DSF and gauge charge spectrum in the PVBS phase exhibit similar dispersive features, but also a distinct continuum along the $q_x = 0$ which is usually related to the fractionalization.[51]

Phase Transition and 't Hooft Anomaly. The PVBS and SF phases break different symmetries, so the phase transition between them should be first-order based on the Ginzburg–Landau theory. However, it also could be continuous due to the deconfinement of the topological defects.[67] Meanwhile, even if it is first-order, the recent work on the checkerboard J-Q model demonstrates the effective gauge field still plays a critical role.[52] Thus, rather than interminable finite size scaling of the ground state, analyzing the features of the spectrum around the phase transition point may provide more clues to the physical mechanism.

While approaching the transition point from the VBS side, the flat band turns to be gapless at (π, π) in

Figs. 3(a)–3(c). Remarkably, the high energy branch at $(0, \pi)$ becomes continuous and falls to zero at the transition point. These exotic features are reminiscent of the deconfined gapless emergent fractional excitations in deconfined quantum phase transitions.[44,46,67] Further from the static structure factor $S^{zz}(\boldsymbol{q}) = \langle |S^z(q)|^2 \rangle$ in Figs. 3(d)–3(f), as the hallmark of translational symmetry breaking, the high intensity at four high symmetry points $(\pm\pi, \pm\pi)$ in PVBS phases changes to be blur at the transition point, and the bow-tie structure indicates the power law correlation with gapless excitations.[5,68] However, the conventional theory of the deconfined quantum criticality based on the "super-spin" with four or more components[32,69,70] can not support an emergent symmetry $\mathrm{U}(1)\times\mathbb{Z}_{2,\mathrm{top}} \to \mathrm{O}(3)$ in which U(1) and $\mathbb{Z}_{2,\mathrm{top}}$ are from SF and PVBS phases, respectively. Then, the deconfined domain wall (point defect) on the domain wall (line defect) arising from the 't Hooft anomaly provides an alternative mechanism[48] for the exotic features observed here.

The effective field theory presents the two fold degeneracy of PVBS phase corresponding to the symmetry breaking of $\mathbb{Z}_{2,\mathrm{top}}$, and they refer to one sublattice of non-crossing plaquette is flippable. When the domain wall excites between two vacua, it can restore the $\mathbb{Z}_{2,\mathrm{top}}$ and break the $\mathcal{C}$ charge conjugation symmetry. Here, the domain wall refers to the pattern with internal degrees of freedom (green regions in Fig. 4), but not the interface between two PVBS patterns (the bottom two rows of green circles and purple circles in the left panel of Fig. 4). Similar to the near-field measurement in the experiment, we make a snapshot of the spin configuration in the PVBS phase which can easily demonstrate the structure in the real space.[71] Then, domain walls can be easily identified once all the flippable non-crossing plaquettes have been determined for a given configuration. As shown in the left panel of Fig. 4, two different kinds of domain walls can be formed between two vacua (PVBS patterns formed by purple circles and green circles), lying horizontally or vertically to minimize the energy.[62] Because all the non-crossing plaquettes in the domain walls are not flippable, the symmetry $\mathbb{Z}_{2,\mathrm{top}}$ is restored. Then turning to the effective electric field picture in the right panel of Fig. 4, the electric fields in the domain walls are polarized (marked with big red arrow). It indicates the domain wall breaks the charge conjugation symmetry because it carries electric flux, and these features are consistent with the analysis of 't Hooft anomaly.[47]

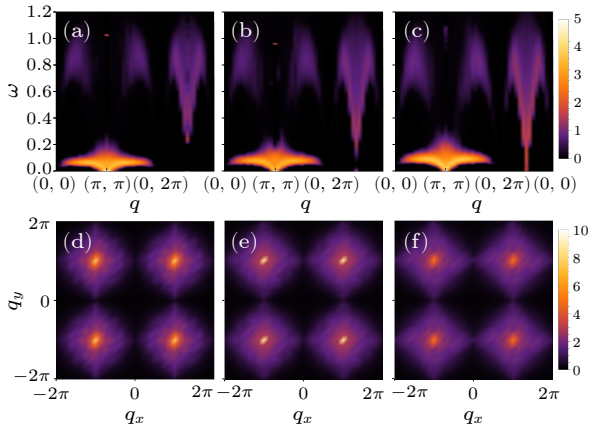

Fig. 3. DSF $S^{zz}(\boldsymbol{q}, \omega)$ (a)–(c) and static structure factor $S^{zz}(\boldsymbol{q})$ (d)–(f) close to the transition point at $t/V = 0.06$, 0.063, and 0.065 from left to right.

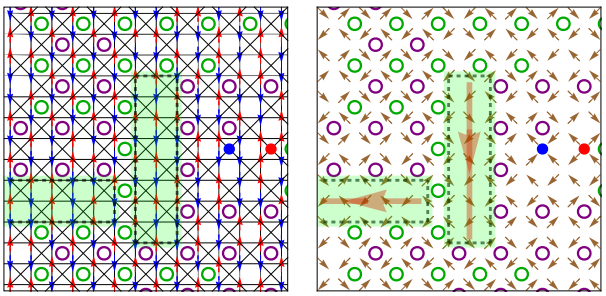

Fig. 4. (Left) The snapshot of the spin configuration obtained from the QMC simulation at $t/V = 0.05$. Spin up and down are represented by red and blue arrows, respectively. The gauge charges are indicated by blue and red solid dots. Purple and green circles denote the flippable non-crossing plaquette. Domain walls are highlighted by green shading. (Right) The corresponding effective electric field representation of the left snapshot. The big red arrow denotes the direction of the electric field in the domain wall.

At the transition point, the snapshot method fails because the domain walls are intertwined with each other. However, the specific directions of domain walls determine that the corresponding part in the spectra should be anisotropic. Meanwhile, the excitations on the domain wall should be gapless and exhibit the characteristics of conformal field theory.[47] Thus, we zoom in the spectra [Fig. 3(c)] at the transition point along $(0, 2\pi) \to (0, 0)$ in the top panel of Fig. 5, and the gapless continuum stays between the two envelope curves (cyan lines) which are the lower and upper boundaries of the two spinon continua of the critical XXZ spin chain.[72] Besides this, we also zoom in on the spectrum in the PVBS phase [Fig. 2(c)] in bottom panel of Fig. 5 along the same path, and the spectrum is also bounded by the lower and upper boundaries of two spinon continua of the XXZ spin chain in the gapped antiferromagnetic phase.[73–75] It seems that the spectrum along this path from PVBS phase to the transition point can be simply modeled by an XXZ spin chain.

The critical theory of XXZ spin chain is the compact boson conformal field theory with $c = 1$, and it matches the prediction of mixed 't Hooft anomaly.[47] Furthermore, another path along $(\pi, 0) \to (0, \pi) \to (\pi, \pi)$ in the middle panel of Fig. 5 demonstrates the continuum is strongly anisotropic, and the closing of the energy gap involves the interplay between the emergent gauge field (flat band) and domain walls. Then at the transition point, although the deconfinement is forbidden in bulk, it can still be allowed on the domain wall. It is noteworthy that this "confinement in the bulk, deconfinement on the wall" phenomenon is also found in the $\mathbb{Z}_2$ VBS phase in the $J-Q_x-Q_y$ model on the square lattice recently.[47,48] In contrast to that, this mechanism serves as an alternative deconfined transition mechanism in our model, and it is natural to expect the enhanced symmetry also exists at this SF-PVBS transition point.

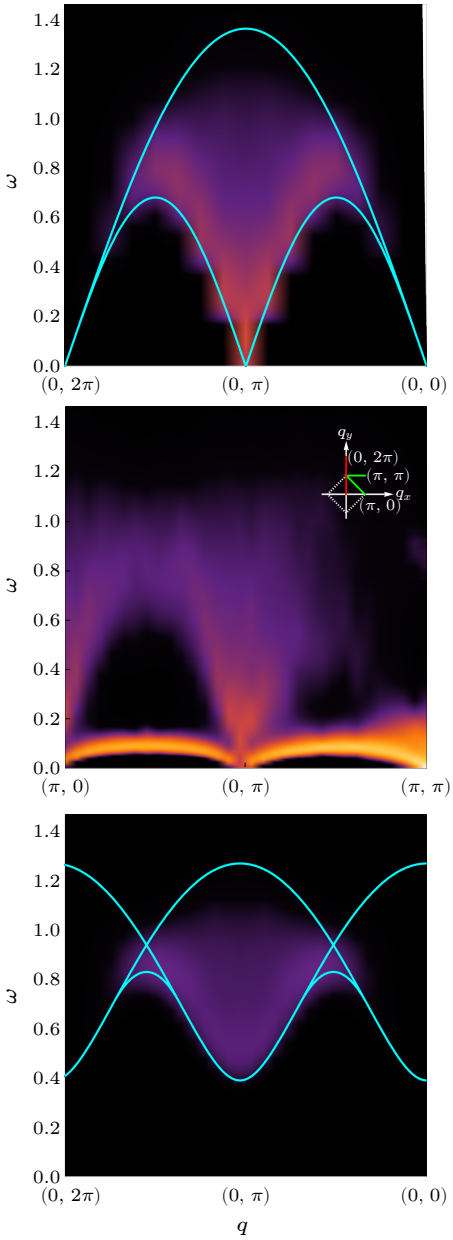

Fig. 5. DSF (top, middle) at the transition point ($t/V = 0.065$), (bottom) with $t/V = 0.05$ along different momentum paths. The cyan lines are fitted by the upper and lower boundaries of two spinon continua of XXZ spin chain. Inset in the middle panel: the red and green lines in the momentum space label the paths of top and middle panel, respectively.

Conclusions. We studied the spectra of the half-filled extended hard-core Bose–Hubbard model (equivalent to the spin-1/2 XXZ model without an external field) on the planar pyrochlore lattice. i) In both the PVBS and SF phases, we observed the fragmentation of the flat band. Through symmetry analysis, we found that the bow-tie flat band is due to the selection rule from certain symmetries. ii) The energy gap is closed at the transition point, and an emergent critical continuum is observed at $(0, \pi)$. The physical mechanism can be understood using the effective Abelian–Higgs model. Consistent with the predictions of previous field-theoretic analysis,[47] many characteristics of the mixed 't Hooft anomaly have been identified through QMC simulations. The domain wall between the two vacua restores the $\mathbb{Z}_{2,\text{top}}$ symmetry, but breaks the charge conjugation symmetry because it must maintain the anomaly. The domain wall appears only in the horizontal or vertical direction, leading to strong anisotropy in the spectra around (π, π). We found a Luttinger liquid-like continuum in the spectra along the $q_x = 0$, suggesting the existence of gapless domain wall excitations on the domain wall. Thus, we propose such deconfinement mechanism may provide an alternative interpretation of the continuous phase transition beyond the Ginzburg–Landau paradigm.

Last but not least, recent rapid advancements in quantum simulation platforms have enabled the study of diverse phenomena in lattice gauge theory. For instance, the kinetics of gauge charges in real space and the static structure factor of transverse field Ising model on a planar pyrochlore lattice have been investigated using superconducting qubits.[18] Additionally, the time evolution of the static structure factor for an XY model[76] has been measured using a Rydberg quantum simulator. Moreover, the one-dimensional topological objects, such as strings, have been explored in multiple quantum simulators, including Rydberg atom arrays,[77] trapped ion systems,[78] and superconducting qubits.[79] We anticipate that quantum simulation setups will soon enable the study of the bow-tie flat band and domain wall configurations as predicted in this work.

Acknowledgements. We thank Yuan Wan, Fa Wang, Long Zhang, Yi-Zhuang You and Changle Liu for helpful discussions. Z.X. is supported by the start-up funding of CQNU (Grant No. 24XLB010). Y.Xu is supported by the Science and Technology Research Program of Chongqing Municipal Education Commission (Grant No. KJQN202100514). X.-F. Z. acknowledges funding from Chongqing Natural Science Foundation under Grant No. CSTB2022NSCQ-JQX0018, the Fundamental Research Funds for the Central Universities Grant No. 2021CDJZYJH-003, and Xiaomi Foundation/Xiaomi Young Talents Program. We acknowledges funding from the National Science Foundation of China under Grant Nos. 12404169, 12147172, 12274046, 11874094, 12147102, and 12347101.

References

[1] Lacroix C, Mendels P, and Mila F 2011 *Introduction to frustrated magnetism: materials, experiments, theory* (Springer Science & Business Media) **164**
[2] Moessner R and Ramirez A P 2006 *Phys. Today* **59** 24
[3] Vojta M 2018 *Rep. Prog. Phys.* **81** 064501
[4] Hermele M, Fisher M P A, and Balents L 2004 *Phys. Rev. B* **69** 064404
[5] Gingras M J P and McClarty P A 2014 *Rep. Prog. Phys.* **77** 056501
[6] Benton O, Sikora O, and Shannon N 2012 *Phys. Rev. B* **86** 075154
[7] Lieb E H 1967 *Phys. Rev. Lett.* **18** 692

[8] Moessner R, Tchernyshyov O, and Sondhi S L 2004 *Journal of Statistical Physics* **116** 755
[9] Wan Y and Tchernyshyov O 2012 *Phys. Rev. Lett.* **108** 247210
[10] Henry L P and Roscilde T 2014 *Phys. Rev. Lett.* **113** 027204
[11] Ralko A, Trousselet F, and Poilblanc D 2010 *Phys. Rev. Lett.* **104** 127203
[12] Shannon N, Misguich G, and Penc K 2004 *Phys. Rev. B* **69** 220403
[13] Pudleiner P and Mielke A 2015 *Eur. Phys. J. B* **88** 207
[14] Wessel S 2012 *Phys. Rev. B* **86** 140501
[15] Glaetzle A W, Dalmonte M, Nath R, Rousochatzakis I, Moessner R, and Zoller P 2014 *Phys. Rev. X* **4** 041037
[16] Ebadi S, Wang T T, Levine H, Keesling A, Semeghini G, Omran A, Bluvstein D, Samajdar R, Pichler H, Ho W W, Choi S, Sachdev S, Greiner M, Vuletić V, and Lukin M D 2021 *Nature* **595** 227
[17] Nisoli C, Moessner R, and Schiffer P 2013 *Rev. Mod. Phys.* **85** 1473
[18] King A D, Nisoli C, Dahl E D, Poulin-Lamarre G, and Lopez-Bezanilla A 2021 *Science* **373** 576
[19] Lieb E, Schultz T, and Mattis D 1961 *Annals of Physics* **16** 407
[20] Oshikawa M 2000 *Phys. Rev. Lett.* **84** 1535
[21] Hastings M B 2004 *Phys. Rev. B* **69** 104431
[22] Watanabe H, Po H C, Vishwanath A, and Zaletel M 2015 *Proc. Natl. Acad. Sci. U.S.A.* **112** 14551
[23] Po H C, Watanabe H, Jian C M, and Zaletel M P 2017 *Phys. Rev. Lett.* **119** 127202
[24] 't Hooft G 1980 *Naturalness, chiral symmetry, and spontaneous chiral symmetry breaking* (Springer) p. 135
[25] Cho G Y, Hsieh C T, and Ryu S 2017 *Phys. Rev. B* **96** 195105
[26] Metlitski M A and Thorngren R 2018 *Phys. Rev. B* **98** 085140
[27] Jian C M, Bi Z, and Xu C 2018 *Phys. Rev. B* **97** 054412
[28] Sulejmanpasic T and Tanizaki Y 2018 *Phys. Rev. B* **97** 144201
[29] Cheng M, Zaletel M, Barkeshli M, Vishwanath A, and Bonderson P 2016 *Phys. Rev. X* **6** 041068
[30] Cheng M and Seiberg N 2023 *SciPost Phys.* **15** 051
[31] Senthil T 2024 *50 Years of the Renormalization Group* p. 169
[32] Wang C, Nahum A, Metlitski M A, Xu C, and Senthil T 2017 *Phys. Rev. X* **7** 031051
[33] Zou L, He Y C, and Wang C 2021 *Phys. Rev. X* **11** 031043
[34] Ye W, Guo M, He Y C, Wang C, and Zou L 2022 *SciPost Phys.* **13** 066
[35] Wen X G 2013 *Phys. Rev. D* **88** 045013
[36] Wen X G 2015 *Phys. Rev. B* **91** 205101
[37] Wang J, Wen X G, and Witten E 2018 *Phys. Rev. X* **8** 031048
[38] Shao H, Qin Y Q, Capponi S, Chesi S, Meng Z Y, and Sandvik A W 2017 *Phys. Rev. X* **7** 041072
[39] Shao H and Sandvik A W 2023 *Phys. Rep.* **1003** 1
[40] Castro Neto A H, Pujol P, and Fradkin E 2006 *Phys. Rev. B* **74** 024302
[41] Tschirsich F, Montangero S, and Dalmonte M 2019 *SciPost Phys.* **6** 028
[42] Ran X, Yan Z, Wang Y C, Rong J, Qi Y, and Meng Z Y 2023 *Phys. Rev. B* **107** 125134
[43] Polyakov A M 1977 *Nucl. Phys. B* **120** 429
[44] Zhang X F, He Y C, Eggert S, Moessner R, and Pollmann F 2018 *Phys. Rev. Lett.* **120** 115702
[45] Senthil T, Balents L, Sachdev S, Vishwanath A, and Fisher M P A 2004 *Phys. Rev. B* **70** 144407
[46] Ma N, Sun G Y, You Y Z, Xu C, Vishwanath A, Sandvik A W, and Meng Z Y 2018 *Phys. Rev. B* **98** 174421
[47] Komargodski Z, Sulejmanpasic T, and Ünsal M 2018 *Phys. Rev. B* **97** 054418
[48] Sulejmanpasic T, Shao H, Sandvik A W, and Ünsal M 2017 *Phys. Rev. Lett.* **119** 091601
[49] Callan C G and Harvey J A 1985 *Nucl. Phys. B* **250** 427
[50] Sandvik A W 2016 *Phys. Rev. E* **94** 063308
[51] Han T H, Helton J S, Chu S, Nocera D G, Rodriguez-Rivera J A, Broholm C, and Lee Y S 2012 *Nature* **492** 406
[52] Zhao B, Weinberg P, and Sandvik A W 2019 *Nat. Phys.* **15** 678
[53] Sun G Y, Wang Y C, Fang C, Qi Y, Cheng M, and Meng Z Y 2018 *Phys. Rev. Lett.* **121** 077201
[54] Becker J and Wessel S 2018 *Phys. Rev. Lett.* **121** 077202
[55] Murthy G, Arovas D, and Auerbach A 1997 *Phys. Rev. B* **55** 3104
[56] Igarashi J I and Nagao T 2005 *Phys. Rev. B* **72** 014403
[57] Lee J Y, You Y Z, Sachdev S, and Vishwanath A 2019 *Phys. Rev. X* **9** 041037
[58] Liu C, Li Y D, and Chen G 2018 *Phys. Rev. B* **98** 045119
[59] Harris A B, Kallin C, and Berlinsky A J 1992 *Phys. Rev. B* **45** 2899
[60] Liu D X, Xiong Z, Xu Y, and Zhang X F 2024 *Phys. Rev. B* **109** L140404
[61] Sadrzadeh M and Langari A 2015 *Eur. Phys. J. B* **88** 259
[62] Xiong Z 2023 arXiv:2306.02522 [cond-mat.str-el]
[63] Xiong Z 2023 *Phys. Rev. B* **108** 195107
[64] McGreevy J 2023 *Annu. Rev. Condens. Matter Phys.* **14** 57
[65] Gaiotto D, Kapustin A, Seiberg N, and Willett B 2015 *J. High Energ. Phys.* **2015** 172
[66] Zhou Z, Liu C, Yan Z, Chen Y, and Zhang X F 2022 *npj Quantum Mater.* **7** 60
[67] Senthil T, Vishwanath A, Balents L, Sachdev S, and Fisher M P A 2004 *Science* **303** 1490
[68] Henley C L 2010 *Annu. Rev. Condens. Matter Phys.* **1** 179
[69] Senthil T and Fisher M P A 2006 *Phys. Rev. B* **74** 064405
[70] Nahum A, Serna P, Chalker J T, Ortuño M, and Somoza A M 2015 *Phys. Rev. Lett.* **115** 267203
[71] Zhang X F and Eggert S 2013 *Phys. Rev. Lett.* **111** 147201
[72] Caux J S, Konno H, Sorrell M, and Weston R 2011 *Phys. Rev. Lett.* **106** 217203
[73] Bougourzi A H, Karbach M, and Müller G 1998 *Phys. Rev. B* **57** 11429
[74] Castillo I P 2020 arXiv:2005.10729 [cond-mat.str-el]
[75] Caux J S, Mossel J, and Castillo I P 2008 *J. Stat. Mech.* **2008** P08006
[76] Chen C, Emperauger G, Bornet G, Caleca F, Gély B, Bintz M, Chatterjee S, Liu V, Barredo D, Yao N Y *et al.* 2023 arXiv:2311.11726 [cond-mat.quant-gas]
[77] Gonzalez-Cuadra D, Hamdan M, Zache T V, Braverman B, Kornjaca M, Lukin A, Cantu S H, Liu F, Wang S T, Keesling A *et al.* 2024 arXiv:2410.16558 [quant-ph]
[78] Liu Y, Zhang W Y, Zhu Z H, He M G, Yuan Z S, and Pan J W 2024 arXiv:2411.15443 [cond-mat.quant-gas]
[79] Cochran T A, Jobst B, Rosenberg E, Lensky Y D, Gyawali G, Eassa N, Will M, Abanin D, Acharya R, Beni L A *et al.* 2024 arXiv:2409.17142 [quant-ph]